Laser-induced graphene/PDMS composite with a dual structure enabling high-sensitivity under micro-strain and extended-range sensing

Guangmeng Chen, Ming Mu, Wenjie Yu, Li Jia, Ziqiang Hu, Weiwei Zhao, Xiaoqing Liu**

State Key Laboratory of Advanced Marine Materials, Ningbo Institute of Materials Technology and Engineering, Chinese Academy of Sciences, Ningbo, Zhejiang 315201, China

Corresponding authors:

Weiwei Zhao, E-mail address: zhaoweiwei@nimte.ac.cn

Xiaoqing Liu, E-mail address: liuxq@nimte.ac.cn

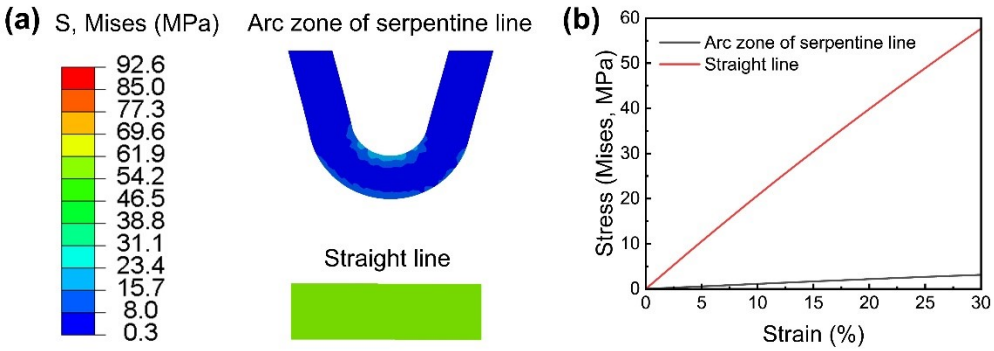

Figure S1. (a) Enlarged view of the finite element simulation results for parallel-connected sensor at the strain of 30%. (b) The Mises stress-strain curves of arc zone at neutral plane for serpentine line and straight line. Upon stretched, the arc zone for serpentine line undergoes bending deformation. The LIG bears a low bending stress near the neutral plane, which ensures the integrity of the conductive structure. For straight line, it undergoes tensile deformation, which results in the rapid increase of tensile stress, causing easy formation of mircocracks.

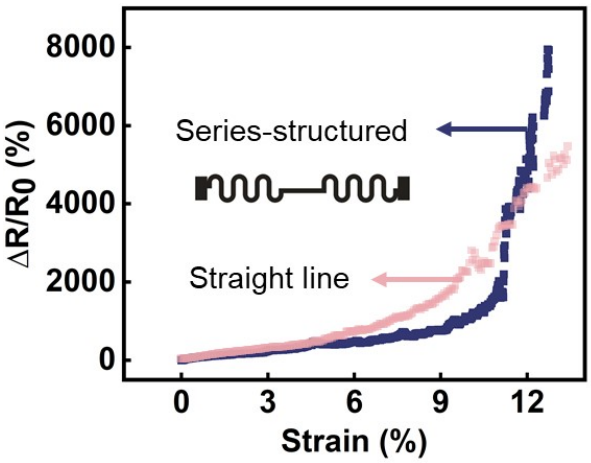

Figure S2. Relationship between the relative resistance changes and strains for the sensor with straight line and the sensor with the series-structure of straight line and serpentine lines

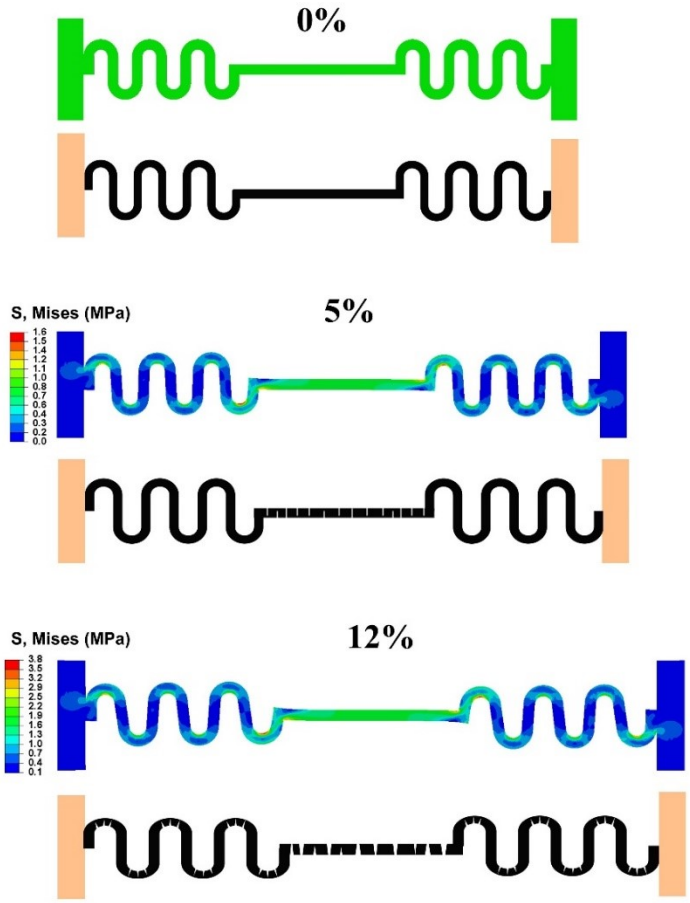

Figure S3. Finite element simulation showing the stress distribution of series-connected sensor at the strain of 0%, 5% and 12%.

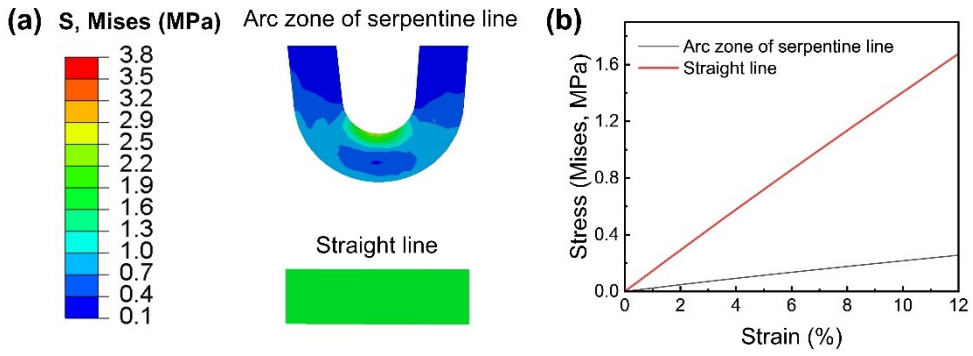

Figure S4. (a) Enlarged view of the finite element simulation results for series-connected sensor at the strain of 12%. (b) The Mises stress-strain curves of arc zone at neutral plane for serpentine line and straight line.

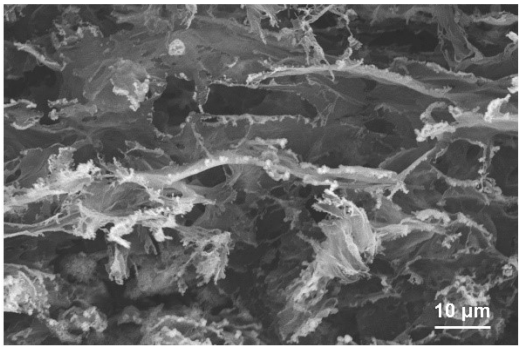

Figure S5. The SEM image showing the pore structure of LIG.

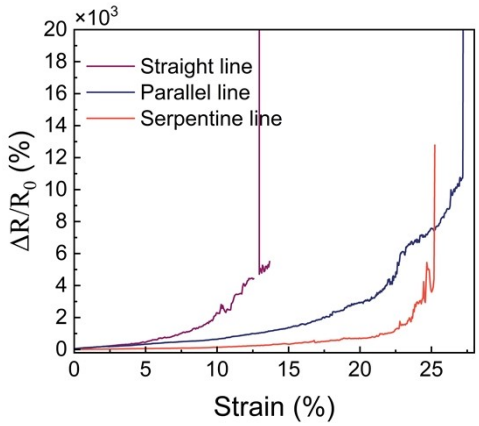

Figure S6. Relationship between relative resistance changes and strains until breakage for straight, serpentine, and parallel lines

Table S1. Comparison of the sensitivity and work range for reported stretchable strain sensors with different conductive fillers and matrices.

Conductive filler	Matrix	Sensitivity	Work range	Ref.
Pt	PUA	16000	<2%	1
Graphene	PDMS	1037	<2%	2
Carbon black	Rubber	28.4	<20%	3
CNT	PDMS	26.7	<150%	4
Ni/Graphene	PU sponge	36.03	<20%	5
		3360.09	20%~65%	
Graphene belts	Dragon skin	175.16	<34.94%	6
		13278	34.94~55.55%	
CNTs/AgNWs	TPU	4.1	<5%	7
		1005.8	5%~350%	
MXene	Polyester Fabric	9.7	<1%	8
		26.6	1%~3%	
		6.6	3%~8%	
MXene/CNT	PDMS	16	<40%	9
		165	40~85%	
		1939	85%~105%	

References

[1] B. Park, J. Kim, D. Kang, C. Jeong, K. S. Kim, J. U. Kim, P. J. Yoo, T. I. Kim, *Adv. Mater.* 2016, **28**, 8130-8137.

[2] X. M. Li, T. T. Yang, Y. Yang, J. Zhu, L. Li, F. E. Alam, X. Li, K. L. Wang, H. Y. Cheng, C. T. Lin, Y. Fang, H. W. Zhu, *Adv. Funct. Mater.* 2016, **26**, 1322-1329.

[3] W. A. Liao, X. J. Wu, Y. Q. Qiu, T. Li, Y. D. Hu, C. Lu, F. Wang, X. L. Liu, *J. Colloid Interf Sci.* 2025, **683**, 684-693.

[4] D.-H. Joo, M.-S. Kang, S. J. Park, S. A. Yu, W.-T. Park, *Sens. Actuators, A* 2022, **345**, 113775.

[5] F. Han, J. H. Li, S. F. Zhao, Y. Zhang, W. P. Huang, G. P. Zhang, R. Sun, C. P. Wong, *J. Mater. Chem. C* 2017, **5**, 10167-10175.

[6] Y. X. Li, T. Y. He, L. J. Shi, R. R. Wang, J. Sun, *ACS Appl. Mater. Interfaces* 2020, **12**, 17691-17698.

[7] G. Li, Y. S. Xue, H. Peng, W. F. Qin, B. Zhou, X. Zhao, G. C. Liu, S. Y. Li, R. H. Guo, *Sens. Actuators, A* 2024, **366**, 114998.

[8] W. Lu, B. Mustafa, Z. Wang, F. Lian, G. Yu, *Nanomaterials (Basel)* 2022, **12**.

[9] B. Xu, F. Ye, R. Chen, X. Luo, G. Chang, R. Li, *Ceramics International* 2022, **48**, 10220-10226.